



KAIST
Team MR²

Team Lead: Jung Myungwoo (mwhasanid@kaist.ac.kr)

Submitted On: Feb 28, 2025

Core Rover Systems

Mechanical System

The rover has four 3D printed TPU wheels, each housing an in-wheel BLDC motor. Each wheel can rotate around the z axis via a Dynamixel RX-64 with a 2:1 belt reduction. The wheels are designed with ridges for maximum grip in outdoor environments, and have horizontal slots for automatic disposal of soil during driving. They are attached to the chassis through lightweight aluminum pipes, which also serves as a pathway for wires to pass through. The left and right wheel assemblies are connected by an averaging mechanism to overcome large obstacles and difficult terrain.

The chassis is constructed from 2020 aluminum extrusion and covered with aluminum sheets to prevent contamination from the elements. Two RTK GPS antennas symmetrically bolted on to the chassis allows operators to accurately pinpoint the rover's position.

To ensure ease of maintenance, a battery door with magnetic fasteners and an access panel with snap fasteners is implemented. This allows the rover operators to quickly swap out batteries or work on the electronics without loosening or tightening any bolts. Alternatively, a charging port can be used to charge the battery via BMS instead of swapping it out. The rover also features a foldable antenna to meet the size requirements, and has an e-stop on its top panel for safety.

Electrical System

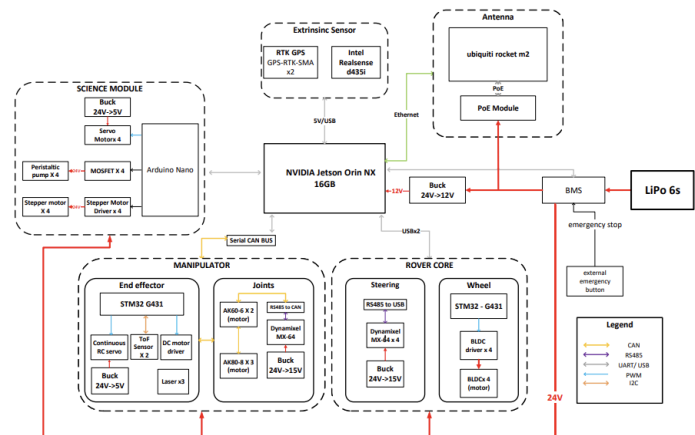
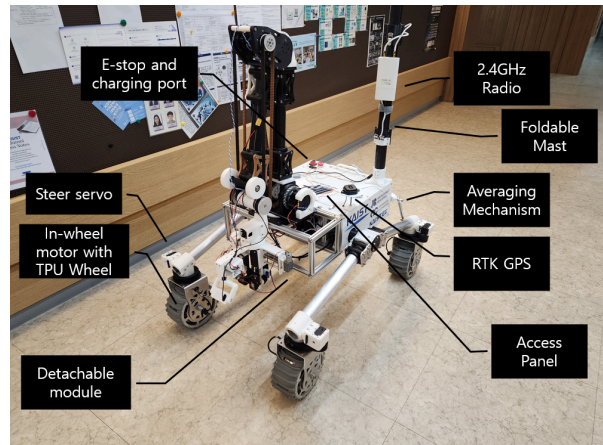
The rover's drive system consists of four BLDC motors for movement and four steering motors, delivering power through a dedicated drive circuit. An MCU-based real-time feedback system precisely controls the rover's speed, and an electric braking system ensures rapid stops when necessary. This drive system employs a custom UART packet protocol for fast and reliable data transmission. Steering motors are controlled via the RS485 protocol, featuring a 5.3 Nm torque rating with a 2:1 reduction gearbox.

The electronic system is powered by a single 6S LiPo battery, which supplies various DC link voltages through multiple DC/DC converters.

A Battery Management System (BMS) monitors overcurrent and overvoltage conditions, tracks battery voltage, remaining capacity, and current consumption in real-time, and transmits this data to the onboard mini-PC via UART. This information is displayed on a dashboard for remote operators. An emergency stop (ESTOP) function is incorporated for rapid response to critical situations, while sensors continuously monitor the circuit and environmental temperature to ensure the system's reliability.

This integrated electrical and control architecture enables the rover to operate efficiently in diverse and complex mission scenarios.

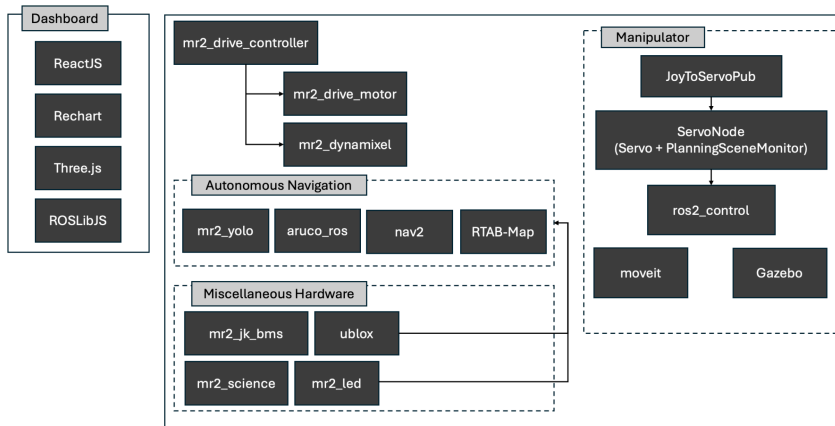
Communications System



The communications system utilizes a 2.4 GHz point-to-point connection, supporting up to 100 Mbps of bandwidth. The rover is equipped with an omnidirectional MIMO antenna, while the base station employs a directional MIMO antenna to maximize reliability and performance. The directional antenna continuously tracks the rover, ensuring uninterrupted signal reception. Moreover, a LoRa-based backup communication protocol is planned for additional redundancy in the network.

User Interface and Software

The dashboard system is built using ROSLibJS in combination with the Tauri Framework, ensuring cross-platform compatibility as well as providing access to low-level, bare-metal features. The integration of React components allows us to harness the vast web ecosystem, incorporating libraries such as Rechart, three.js, and Gamepad API, among others. Meanwhile, helper functions written in Rust enable direct interaction with system-level functionalities, including sending IGMP ping packets and Wake-on-LAN commands. Furthermore, Rust and Tauri provide a minimal memory footprint, fast execution, and enhanced memory safety, effectively eliminating common memory bugs.



The user interface is thoughtfully organized into multiple tabs, each dedicated to core utilities such as Overview, Driving, Science, and Debugging. This segmentation allows users to navigate between different operational aspects of the system with ease. Real-time updates are provided for all nodes, topics, and logs, ensuring immediate access to critical system information. Additionally, a variety of debug menus are available to support hardware maintenance, offering an accessible alternative for users who may not be comfortable with command-line interfaces.

Complementing these features, the system streams video feeds through `web_video_server`, allowing real-time monitoring of various camera inputs directly from the dashboard. This provides users with instant visual feedback and situational awareness. Additionally, the dashboard includes a 3D model visualization of the current status of the science module, offering an intuitive and interactive representation of the module's operational state and spatial configuration.

Another key feature of the dashboard is the interactive map user interface, which allows users to add, delete, and edit waypoints dynamically. This functionality provides a hands-on approach to mission planning and route adjustments, ensuring that operators can efficiently modify paths in real time based on mission needs or changing conditions.

Approach to Competition Missions

Extreme Delivery and Equipment Servicing

To effectively carry out extreme delivery and equipment servicing missions, the rover is equipped with an 8-DOF manipulator with a 2-DOF end effector system. To minimize inertia, actuators are positioned close to the main body. Actuators for joints 1 to 3 are placed near the base, while actuators for joints 4 and 5 are located near joint 3, or the 'elbow'. Since the range of motion for joint 3 is

primarily 0 to -180 degrees, an offset hinge structure is applied to maximize its workspace. A belt drive is used for power transmission, and a differential mechanism is integrated into the joint 4 and 5 sections. Additionally, to reduce the length of the link connecting joint 3 and joint 4, motors for joints 4 and 5 are mounted perpendicular to the link.

The actuators for joints 1 to 5 are built using Cubemars robot servos. Joints 1 to 3 utilize the CubeMars Ak80-8, which provides a maximum torque of 25 Nm and a continuous torque of 10 Nm with a reduction ratio of 8. Joint 1 directly connects to the Ak80-8, whereas joints 2 and 3, requiring higher torque, incorporate additional reduction systems. Joint 2 uses a custom 3K compound planetary drive with a 49.38:1 reduction ratio, while joint 3 employs a dual-stacked planetary drive, achieving an overall 16:1 reduction ratio through two 4:1 stages. For joints 4 and 5, the CubeMars Ak60-6 is used, which has a maximum torque of 9 Nm, a continuous torque of 3 Nm, and a reduction ratio of 6. Further reduction of 42:26 is applied through the belt drive system.

To achieve maximum gripping strength, the end effector employs a parallel gripper mechanism driven by a lead screw attached to a geared DC motor. Two grating lasers assist in positioning the gripper. For operating switches and keyboards, a small rack and pinion mechanism, driven by a continuous RC servo motor, is implemented. A point laser is placed at the front of the mechanism to indicate its target position. Additionally, two ToF sensors aid in aligning the end effector parallel to the lander panel during equipment servicing.

An STM32 microcontroller is housed within the end effector, communicating with the main PC via a CAN bus to ensure ease of wiring and modularity. It receives commands to control the gripper and rack & pinion mechanism's speed and position while also transmitting ToF sensor data to the main PC.

The entire robotic system integrates a CAN bus network from joint 1 to the end effector, ensuring high modularity and scalability, allowing for flexible adaptation to diverse mission requirements. Furthermore, the manipulator is integrated with ROS 2's MoveIt simulation, receiving real-time joint velocity and position data. The control system employs Jacobian-based control for precise joint positioning, speed control, collision detection, and trajectory planning. Additionally, a joystick control function is included for manual operation. This integrated system guarantees high stability and efficiency, even in complex operational environments. Two cameras displaced 90 degrees from each other help position the end effector during delivery and equipment servicing.

The aforementioned steering system allows the rover to drive in both ackerman steering and holonomic driving, and the averaging mechanism along with the ridged wheels allow the rover to overcome obstacles. The high gear ratio of the manipulator allows the rover to pick up heavy payloads for delivery, and the ROS2 MoveIt framework used with the laser and camera system allows precise positioning of the manipulator to perform equipment servicing.

For the autonomous keyboard service mission, the system treats the wall-mounted keyboard as a decal, matching keypoints from the live camera stream to a reference keyboard image. A closed-loop controller tracks the laser mark on the end effector, ensuring precise keypressing. This approach combines robust visual tracking with precise control, enabling accurate and reliable keyboard interaction in real-time.

Autonomous Navigation

For autonomous missions, a multi-sensor approach is employed to ensure a robust and capable system. Two ZED-F9P RTK GPS modules are mounted on the left and right sides of the rover's body, providing centimeter-level positioning accuracy. These modules communicate with the main onboard computer via the UBX protocol over UART, while RTK correction data from a base station is transmitted using a Rocket M2 network interface via a self-hosted NTRIP server.

Beyond GPS, a Realsense D435i camera provides an RGB-D video stream along with IMU data. The system fuses data from the dual RTK modules, IMU, and visual odometry using the RTAB-MAP SLAM toolkit, which constructs an occupancy grid for localization and mapping. This occupancy grid is then fed

into the Nav2 module for dynamic path planning.

To enhance navigation, Aruco markers are detected using an OpenCV-based node, generating waypoints for precise navigation. Additionally, a YOLO 11n model trained on 8,000 images of orange rubber mallets and plastic bottles is integrated into a ROS 2 node. This model generates waypoints based on object detection, similar to the Aruco marker node.

Testing and Operations

From the early stages of the project, the team first built a prototype to validate the suspension and steering structure, which forms the foundation of the rover's driving mechanism. Through repeated off-road tests, the optimal angle for the averaging mechanism was determined to be approximately 15°. We also found that a gear-based reduction mechanism for steering was prone to backlash, so we utilized a timing belt and pulley system to tackle this issue. Subsequent full-scale driving tests confirmed sufficient chassis rigidity, allowing us to significantly reduce the thickness of aluminum pipes and profiles to lighten the rover. Replacing solid tires with 3D-printed TPU tires significantly reduced wheel weight while maintaining shock absorption performance.

Along with the development of a new rover based on these improvements, the manipulator and science module were developed in parallel. The manipulator focused on resolving belt skip issues and improving the durability of 3D-printed parts. Future plans include scenario tests to validate repeated joint movements and heavy load handling performance.

The communication quality was also validated in various outdoor environments. By varying the distance between the rover and the ground control station and intentionally creating non-line-of-sight (NLoS) conditions, we measured latency and signal strength. The results showed that latency could range from a few seconds to tens of seconds behind obstacles. To address this, we are researching a drone relay system. By having a drone hover and act as a relay node, the rover's signal can be transmitted through the drone to establish a direct line of sight with the base station, improving link quality. This approach is expected to mitigate signal blockages caused by terrain and obstacles, serving as a key strategy for maintaining stable control commands and data streams.

Additionally, after individual subsystems (suspension, steering, drivetrain, manipulator, science module, etc.) passed their respective performance tests, an integrated test was conducted to verify the organic operation of the entire system. Initially, joint tests were performed in a controlled indoor environment before gradually expanding to outdoor conditions resembling real mission scenarios, such as loose sand, rocky terrain, and steep slopes. The results demonstrated that all systems operated reliably under high-stress conditions and that the rover maintained sufficient driving stability and control even on irregular surfaces. Special attention was given to vibrations and interference caused by the manipulator, and improvements are being identified at both the design and software levels.

Team Development

Internally, the team combined new member training with test driving to enhance operational capabilities. Senior team members conducted small seminars and practical sessions covering topics such as mechanical design (Fusion360, SolidWorks), MCU feedback and communication protocols (RS485, CAN), BMS control, as well as ROS2 and manipulator control algorithms. During the development of the science module, KiCad was used to design PCBs, improving the team's understanding of electronic circuits.

Once the rover reached a sufficient level of completion, demonstration drives were conducted at various campus locations to showcase its operation to both new and existing students, gathering immediate feedback. This process was more than just a promotional effort; it provided an opportunity to observe how the rover responded to unexpected user interactions and external factors. Moving forward, the team plans to continue conducting integrated tests in diverse outdoor environments under near-mission conditions to identify and address issues while enhancing team members' expertise.

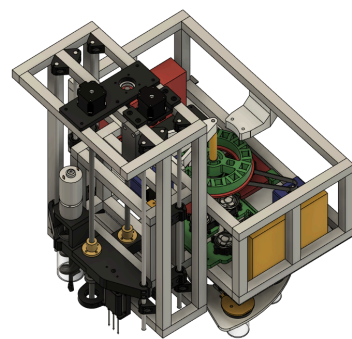
Gantt chart and Project Budget Table:

Task #	Task Name	Research and Planning				Design Phase				Building and Testing				Competition Preparing Phase							
		September		October		November		December		January		February		March		April		May			
		1	2	3	4	1	2	3	4	1	2	3	4	1	2	3	4	1	2	3	4
1	Drivetrain																				
1.1	Research on components																				
1.2	Purchasing components																				
1.3	Chassis design																				
1.4	Suspension & steering design																				
1.5	Manufacturing & Assembly																				
1.6	Refining Design																				
1.7	Testing and drive practice																				
2	Manipulator																				
2.1	Researching robot actuators																				
2.2	Selecting and purchasing components																				
2.3	J1~J3 design																				
2.4	J4~J6, end effector design																				
2.5	Manufacturing & Assembly																				
2.6	Refining Design																				
2.7	Testing and control practice																				
3	Science Module																				
3.1	Life detection method research																				
3.2	researching lab equipment																				
3.3	Onboard lab design																				
3.4	Manufacturing																				
3.5	Assembly																				
3.6	Assessment of results																				
3.7	Refining design																				
4	Electronics																				
4.1	Research on power circuits																				
4.2	Research on motor drivers																				
4.3	Testing with development boards																				
4.4	low level firmware development																				
4.5	PCB design and fabrication																				
4.6	PCB design iteration																				
4.7	Low level firmware refinement																				
5	Autonomous Driving																				
5.1	Researching navigation algorithms																				
5.2	Researching and testing sensors																				
5.3	Testing radio communication																				
5.4	Developing ROS2 packages																				
5.5	Application development																				
5.6	Real world testing																				
5.7	Tuning parameters																				

Template Work Breakdown Structure Financial Report			
Team Name: My Team			
WBS #	Description	Item Total Cost*	System Total Cost*
0	TOTAL ROVER COST		\$8,781.95
1	ROVER FRAME, SUSPENSION, AND CHASSIS		\$530.29
1.1	Frame		
1.1.1	2020 Aluminum Extrusion	\$62.24	
1.1.2	Aluminum Panels & Powder coating	\$152.55	
1.1.3	Assorted Bolts	\$84.42	
1.2	Wheel-leg assembly		
1.2.1	TPU filament	\$28.73	
1.2.2	Wheel holder bracket	\$90.30	
1.2.3	aluminum pipe	\$29.96	
1.2.4	PLA filament	\$82.09	
2	DRIVE AND ENERGY SYSTEM		\$1,828.30
2.1	Motor/Wheel Assemblies		
2.1.1	Scooter motor	\$112.33	
2.2	Motor Drivers/Controllers		
2.2.1	Motor Drivers	\$361.23	
2.2.2	Steering Servo motor	\$552.11	
2.3	Energy/Power Components		
2.3.1	Lithium-Polymer Batteries	\$280.92	
2.3.2	PCB	\$41.23	
2.3.3	Kit Switch	\$12.45	
2.3.4	Battery Monitoring Circuit	\$82.34	
2.3.5	DC-to-DC Converter	\$112.53	
2.3.6	Assorted Wiring	\$205.09	
2.3.7	Assorted Connectors	\$68.07	
3	ELECTRONICS AND ON-BOARD PROCESSING		
3.1	On-board Processing/Computers		
3.1.1	Jalson otti mx	\$1,200.00	\$2,025.00
3.1.2	MCU	\$70.00	
3.2	Sensors		
3.2.1	Cameras	\$200.00	
3.2.2	SLAM camera	\$550.00	
3.2.3	ToF sensors	\$5.00	
4	COMMAND & CONTROL, AND COMMUNICATIONS SYSTEM		
4.1	Rover Node Communications		
4.1.1	Antenna	\$80.00	\$1,038.00
4.1.2	Router	\$75.00	
4.1.3	PoE	\$100.00	
4.1.4	RTK gps	\$546.00	
4.2	Base Station Communications		
4.2.1	Antenna	\$100.00	
4.2.1	Trippod	\$90.00	
4.3	Command & Control Systems		
4.3.1	Xbox controller	\$50.00	
4.3.2	UART to USB	\$15.00	
4.3.3	RS485 to USB	\$22.00	
5	ARM SYSTEM		
5.1	Arm Mechanical Frame		
5.1.1	Belts and pulleys	\$289.37	\$3,165.37
5.1.2	Linear Shafts	\$300.00	
5.1.3	Gears	\$125.00	
5.1.4	Carbon Fiber Pipe		
5.2	Arm Electrical and Controls		
5.2.1	AK 80-8 (J1-J3)	\$1,650.00	
5.2.2	AK 60-6 (J4-J5)	\$600.00	
5.2.3	Servo Motor (J6)	\$197.00	
5.2.4	CAN to USB	\$20.00	
5.3	Gripper		
5.3.1	Servo Motor	\$4.00	
5.3.2	LASER	\$40.00	
5.3.3	Part		
6	SCIENCE PAYLOAD		
6.1	Sample Collection Subsystem		
6.1.1	2020 aluminum extrusion	\$47.89	\$194.99
6.1.2	acrylic pipe	\$4.79	
6.1.3	auger drill	\$12.31	
6.2	On-board Science Sensors		
6.2.1	Moisture & Temperature sensor		
6.2.2	Part		
6.3	Actuators		
6.3.1	Stepper motors	\$120.00	
6.3.2	servo motors	\$10.00	
7	MISCELLANEOUS PARTS		

SAR Science Plan:

Our MR2 team has focused on life detection in our science mission. The science module includes a downward facing camera for analyzing geological features, a camera for creating panoramas and stratigraphic profiles, a drill, a temperature/humidity sensor, four caches for sample storage, several peristaltic pumps, a 12-slot cuvette holder, and a UV-VIS spectrophotometer. Samples will be collected and analyzed from two sites, and three life detection experiments will be performed. The geological characteristics of the MDRS region were referenced from “The Regolith Geology of the MDRS Study Area” [1] and “MDRS Expedition Guide” [2]. Clastic rocks like siltstone and shale show signs of past water activity such as cracking and stratification which we use to select sites.



Using the downward facing camera, we identify two locations with visible cracks and traces of water. At each site, two types of samples are collected: the first is stored in a cache (a beaker with a 3D printed lid) for transport, and the second is mixed with water via a peristaltic pump. The upper layer of the soil water mixture is then transferred into a cuvette to minimize optical interference from scattered light by soil particles.

Of the three life detection methods, two use protein detection reagents. To ensure high accuracy within our limited time, we conducted preliminary tests with egg albumin and four different well known protein detection reagents; Biuret, Lowry, Ninhydrin and Bradford. We reacted egg albumin solutions of increasing concentration with reagents and analyzed the linearity between concentration and absorbance using Origin 2025. For the Biuret reaction, 0.1%–1% egg albumin solutions were measured at 540 nm, yielding an adjusted R^2 of 0.89. This method is fast and simple. The Lori reaction, measured at 620 nm, showed linearity in the 0.005%–0.009% range but requires a waiting period after mixing, so it was excluded. The Ninhydrin reaction was also excluded due to its lower accuracy and the need for heating, which is impractical with our fixed spectrophotometer and rotating cuvette holder. The Bradford reaction, measured at 595 nm, produced an adjusted R^2 of 0.74 with excellent speed and sensitivity, so we adopted it along with the Biuret test. These results, as supported by “Influence of Soil Parameters...” [4] and “A simple biochemical method...” [3], indicate that both methods are suitable for detecting trace proteins in soil. Thus, our protein detection experiments use both the Biuret and Bradford methods; the samples are pre stored in cuvettes for transport, mixed with the supernatant of the soil–water mixture, and then analyzed.

The third life detection method is UV-VIS spectral scanning. Distilled water is used as the solvent to measure absorbance from 200 to 1000 nm, and the peaks are analyzed to identify metabolic byproducts. Above 300 nm, an exponential increase in absorbance is observed due to scattering by residual soil particles. This scattering, which increases proportionally with particle size and wavelength, is explained by Mie scattering theory (Bohren & Huffman[6]) and fits an exponential function with an adjusted R^2 above 0.95. Peaks at 210, 225, 230, 245, 270, and 285 nm were observed, and “UV Visible Spectroscopic...” [5] supports that these peaks correspond to biological metabolic byproducts.

[1] Clarke, J. (2003). The Regolith Geology of the MDRS Study Area; [2] Hargitai, H. I. (Ed.). (2008). MDRS Expedition Guide. Cosmic Materials Space Research Group, Eötvös Loránd University; [3] Li, Y., Collins, D. A., & Grintzalis, K. (2023). A simple biochemical method for the detection of proteins as biomarkers of life on martian soil simulants and the impact of UV radiation. *Life*, 13(5), 1150. doi:10.3390/life13051150; [4] Olszewska, A., Napora, J., Kamieński, K., Dzierżek, K., Rečko, M., & Kawecki, A. (2020). Influence of Soil Parameters on Protein Presence for a Mars Rover Analogue’s On-Board Laboratory Setup. In 2020 21st International Carpathian Control Conference (ICCC) (pp. 1–6). doi:10.1109/ICCC49264.2020.9257250; [5] Somer, S. M., Brown, J. T., & Williams, K. E. (2022). UV Visible Spectroscopic Identification of Metabolic Byproducts in Martian Soil Analogs. *Planetary and Space Science*, 195, 105–114. doi:10.1016/j.pss.2021.105114; [6] Bohren, C. F., & Huffman, D. R. (1983). *Absorption and Scattering of Light by Small Particles*. Wiley; [7] Batjes, N. H. (2017). International Soil Reference and Information Centre (ISRIC). Wageningen, The Netherlands; [8] Osik, N. A., Zelentsova, E. A., Sharshov, K. A., & Tsentalovich, Y. P. (2022). Nicotinamide adenine dinucleotide reduced (NADH) is a natural UV filter of certain bird lens; [9] Clarke, A. L., & Jennings, A. C. (n.d.). Spectrophotometric Estimation of Nitrate in Soil Using Chromotropic Acid.